Search for cosmic neutrinos with ANTARES

Bogazzi, C.

8. Results

The search for truth is in one way hard and in another easy. For it is evident that no one can master it fully nor miss it wholly. But each adds a little to our knowledge of nature and from all the facts assembled these arise a certain grandeur.

Aristoteles

We present here the results of the two searches introduced in Chapter 7. Since no significant deviations from the background are observed, upper limits are derived. Section 8.1 and 8.2 present the results obtained for the full-sky search and the candidate list search respectively. In Section 8.3, upper limits on the neutrino emission models presented in Chapter 2 are reported.

8.1. Full-sky search

In the full-sky search we look for an excess of signal events everywhere in the visible sky. Starting from the 3058 selected events, the pre-clustering algorithm selects a total of 1413 clusters with at least 4 events within a cone of 3 degrees diameter. Figure 8.1 shows a sky map in equatorial coordinates of $\mathcal{Q}(\alpha, \delta)$.

Similarly, Figure 8.2 shows the sky map of pre-trial significances, i.e. the penalty factor due to the fact that we look at many points in the sky is not taken into account.

The most significant deviation from the background (or "hot-spot") is located at $(\alpha, \delta) = (-46.5^\circ, -65.0^\circ)$ where 5(9) events are within 1(3) degrees of this position. The corresponding cluster of events is shown in Figure 8.3. The maximum likelihood fit assigns $\mu_s = 5.1$ and the value of the test statistic is $\mathcal{Q} = 13.1$. The pre-trial p-value is 4.4 $\times 10^{-3}$.

Comparing the observed test statistic with the $\mathcal{Q}$ distribution for the background only hypothesis (see Figure 7.14), yields a post-trial[1] p-value of 2.6% which is equivalent to 2.2σ (adopting the two-sided convention). Therefore the result obtained is compatible with a statistical fluctuation of the background. The equatorial coordinates and other reconstruction parameters for the nine events found in the most signal-like cluster are reported in Table 8.1. Two possible counterparts of the hot-spot were found in the frequency range from radio to X-rays. The closest source is the Active Galactic Nuclei PKS 2047-655

[1] The post-trial p-value is determined as the fraction of pseudo-experiments with at least one cluster with a higher value of the test statistic.

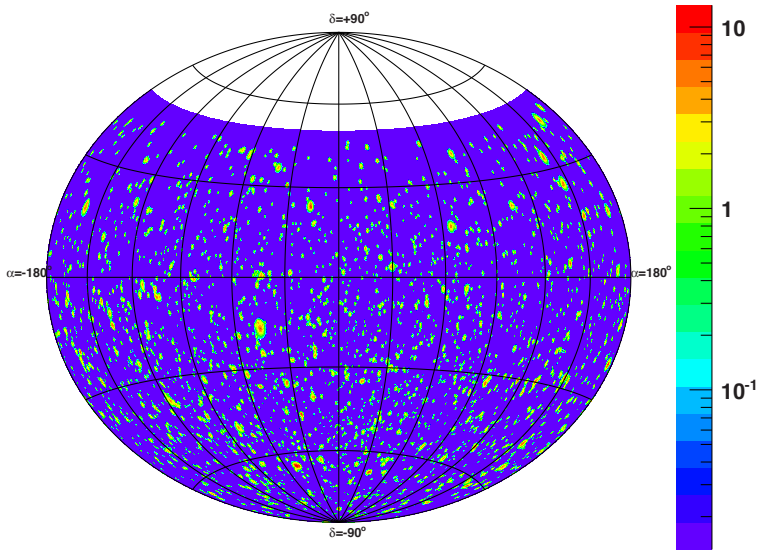

Figure 8.1.: Sky map in equatorial coordinates showing the values of the test statistic obtained for each cluster in the full-sky search.

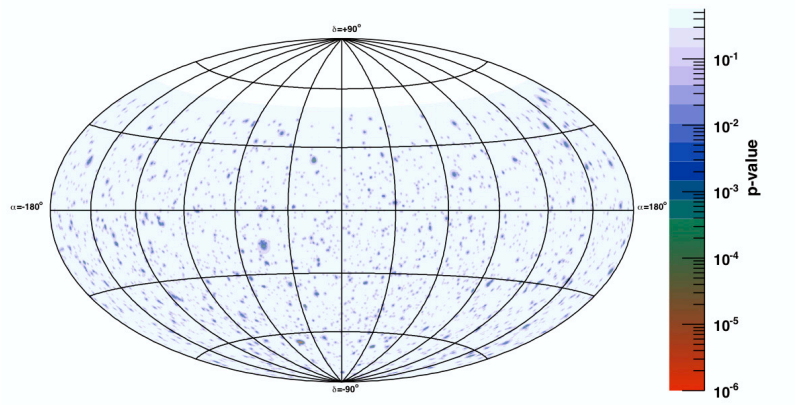

Figure 8.2.: Sky map in equatorial coordinates showing the pre-trial p-values obtained in the full-sky search.

located at a distance of 0.54 degrees from the center of the cluster (redshift $z = 2.3$). The other possible counterpart is the galaxy cluster AC 103 located at redshift $z = 0.31$ at a distance of 0.87 degrees from the center of the cluster.

The second most signal-like cluster is located at $(\alpha, \delta) = (-27..2°, -46.0°)$. In this case 7(3) events are within 1(3) degrees of this position. The value of the test statistic

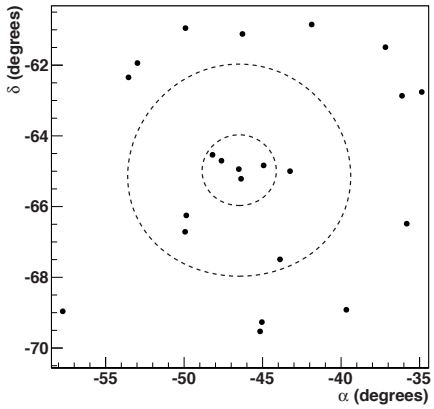

Figure 8.3.: Most signal-like cluster found in the full-sky search with 5(9) events are located within 1(3) degrees of its center.

Run number	α [°]	δ [°]	N_{hits}	Λ	N_{lines}
32168	-46.5	-64.9	56	-4.79	9
43222	-47.2	-64.7	29	-5.06	4
50225	-46.3	-65.2	48	-4.80	8
52092	-44.9	-65.8	125	-4.73	7
53607	-48.2	-64.5	117	-4.68	10
37402	-49.9	-66.7	41	-4.26	5
38431	-49.8	-66.3	34	-5.16	9
43022	-43.9	-67.5	42	-4.99	6
47660	-43.2	-65.0	48	-5.08	9

Table 8.1.: Run number (first column), equatorial coordinates, number of hits used in the reconstruction, value of Λ and number of lines used in the reconstruction (last column) for the nine events of the most signal like cluster in the full-sky search. The line separates the five events which are within 1 degree from the fitted source position.

for this cluster is $\mathcal{Q} = 8.5$ which leads to a post-trial p-value of 0.8.

8.1.1. Multi-wavelength observation of the hot-spot

The ANTARES collaboration have proposed to the H.E.S.S. collaboration to observe the region around $(\alpha, \delta) = (-46.5°, -65.0°)$ in order to search for a possible gamma-ray excess at this location. The H.E.S.S. telescope detects gamma-rays in the 100 GeV - 100 TeV energy range with a field of view of 5 degrees.

A two hour observation was made in November 2012. The data have been taken in so-called "wobble" mode, i.e. the source direction is located with a pointing offset of 0.5°

in declination relative to the center of field of the camera.

The result is shown in Figure 8.4. Unfortunately, no significant excess of gamma-rays was found and an upper limit on the gamma-ray flux was derived [160] and compared with a prediction (red line) obtained by converting the neutrino flux into a flux of gamma-rays. The conversion relies on Monte Carlo simulations and was derived following the assumptions made in [95]. It is likely that the ANTARES excess is due to a background fluctuation.

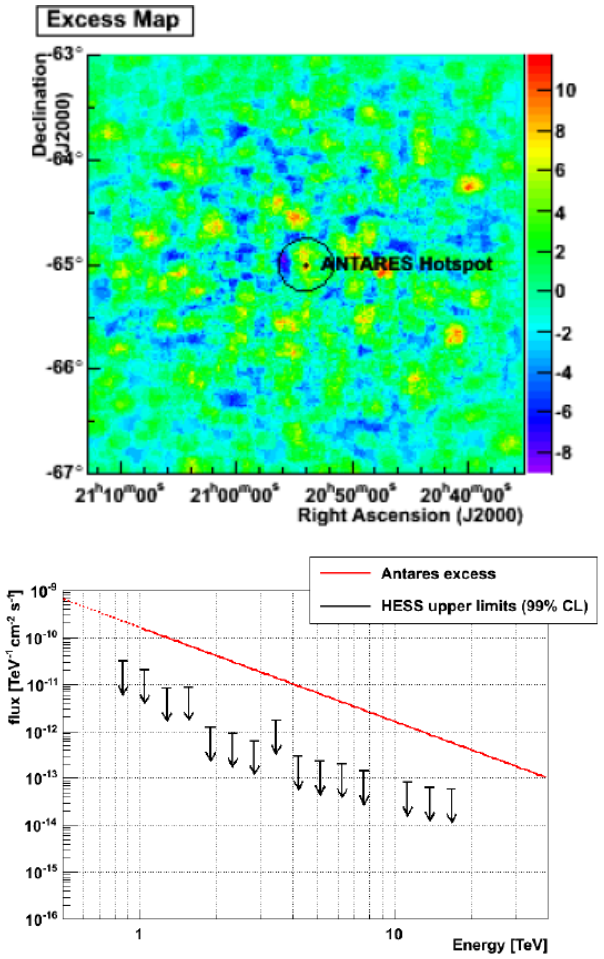

Figure 8.4.: Top: Map of the very high-energy gamma-ray events exceeding the background expectation at the location of the most signal-like cluster found with the full-sky search. Bottom: upper limit on the gamma-ray flux.

8.2. Candidate list search

The results of the candidate list search are reported in Table 8.2 and shown in Figure 8.6. The most signal-like source in the list is HESS J1023-575, a source coincident with the young stellar cluster Westerlund 2. Three events are located within 1 degree from the source as shown in Figure 8.5.

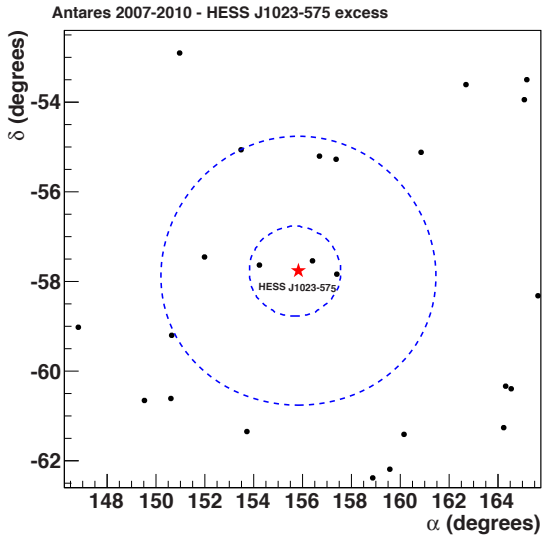

Figure 8.5.: Most signal-like source found in the candidate list search. Three events are within 1 degree from the source. The fit returns $\mu_{\rm s} = 2.0$ with a corresponding test statistic of $\mathcal{Q} = 2.4$, compatible with a background fluctuation.

The fit yields $\mu_{\rm s} = 2.0$ and the corresponding test statistic is $\mathcal{Q} = 2.4$. The probability to have such a fluctuation in one of the candidates in the absence of a signal was determined from pseudo-experiments to be 41%, fully compatible with a background fluctuation. Upper limits at 90% CL, using the FC prescription, are then derived for the normalisation on a neutrino flux proportional to E_ν^{-2} for each of the candidate sources considered. These limits are shown in Figure 8.6. Limits from other neutrino experiments are also indicated. For some sources in the Southern sky the limits set in this analysis are the most restrictive. We remind that for the Southern sky the IceCube detector is more sensitive to ultra high-energy neutrinos with $E_\nu > 1\,\mathrm{PeV}$ [59] which are not relevant for Galactic sources. For this analysis 80% of the signal events has 4 TeV $< E_\nu < 700$ TeV. To illustrate this, the neutrino flux needed for a 5σ discovery as a function of the neutrino energy for both ANTARES and IceCube is shown in Figure 8.7 for three declinations in the Southern sky. It can be seen that the discovery potentials of ANTARES and IceCube cover different energy ranges.

Table 8.2. Results from the search for high-energy neutrinos from sources in the candidate list. The equatorial coordinates $(\alpha_{\rm s}, \delta_{\rm s})$ in degrees, p-value $(\rm p)$ probability and the 90% C.L. upper limit on the E_ν^{-2} flux intensity $\phi^{90\%\rm CL}$ in units of $10^{-8}\rm GeV^{-1}cm^{-2}s^{-1}$ are given (sorted in order of increasing p-value) for the 51 selected sources. When it is not quoted, the p-value is 1.

Source name	$\alpha_s[^\circ]$	$\delta_s[^\circ]$	p	$\phi^{90\%CL}$	Source name	$\alpha_s[^\circ]$	$\delta_s[^\circ]$	p	$\phi^{90\%CL}$
HESS J1023-575	155.83	-57.76	0.41	6.6	SS 433	-72.04	4.98	–	4.6
3C 279	-165.95	-5.79	0.48	10.1	HESS J1614-518	-116.42	-51.82	–	2.0
GX 339-4	-104.30	-48.79	0.72	5.8	RX J1713.7-3946	-101.75	-39.75	–	2.7
Cir X-1	-129.83	-57.17	0.79	5.8	3C454.3	-16.50	16.15	–	5.5
MGRO J1908+06	-73.01	6.27	0.82	10.1	W28	-89.57	-23.34	–	3.4
ESO 139-G12	-95.59	-59.94	0.94	5.4	HESS J0632+057	98.24	5.81	–	4.6
HESS J1356-645	-151.00	-64.50	0.98	5.1	PKS 2155-304	-30.28	-30.22	–	2.7
PKS 0548-322	87.67	-32.27	0.99	7.1	HESS J1741-302	-94.75	-30.20	–	2.7
HESS J1837-069	-80.59	-6.95	0.99	8.0	Centaurus A	-158.64	-43.02	–	2.1
PKS 0454-234	74.27	-23.43	–	7.0	RX J0852.0-4622	133.00	-46.37	–	1.5
IceCube hotspot	75.45	-18.15	–	7.0	1ES 1101-232	165.91	-23.49	–	2.8
PKS 1454-354	-135.64	-35.67	–	5.0	Vela X	128.75	-45.60	–	1.5
RGB J0152+017	28.17	1.79	–	6.3	W51C	-69.25	14.19	–	3.6
Geminga	98.31	17.01	–	7.3	PKS 0426-380	67.17	-37.93	–	1.4
PSR B1259-63	-164.30	-63.83	–	3.0	LS 5039	-83.44	-14.83	–	2.7
PKS 2005-489	-57.63	-48.82	–	2.8	W44	-75.96	1.38	–	3.1
HESS J1616-508	-116.03	-50.97	–	2.7	RCW 86	-139.32	-62.48	–	1.1
HESS J1503-582	-133.54	-58.74	–	2.8	Crab	83.63	22.01	–	4.1
HESS J1632-478	-111.96	-47.82	–	2.6	HESS J1507-622	-133.28	-62.34	–	1.1
H 2356-309	-0.22	-30.63	–	3.9	1ES 0347-121	57.35	-11.99	–	1.9
MSH 15-52	-131.47	-59.16	–	2.6	VER J0648+152	102.20	15.27	–	2.8
Galactic Center	-93.58	-29.01	–	3.8	PKS 0537-441	84.71	-44.08	–	1.3
HESS J1303-631	-164.23	-63.20	–	2.4	HESS J1912+101	-71.79	10.15	–	2.5
HESS J1834-087	-81.31	-8.76	–	4.3	PKS 0235+164	39.66	16.61	–	2.8
PKS 1502+106	-133.90	10.52	–	5.2	IC443	94.21	22.51	–	2.8
					PKS 0727-11	112.58	11.70	–	1.9

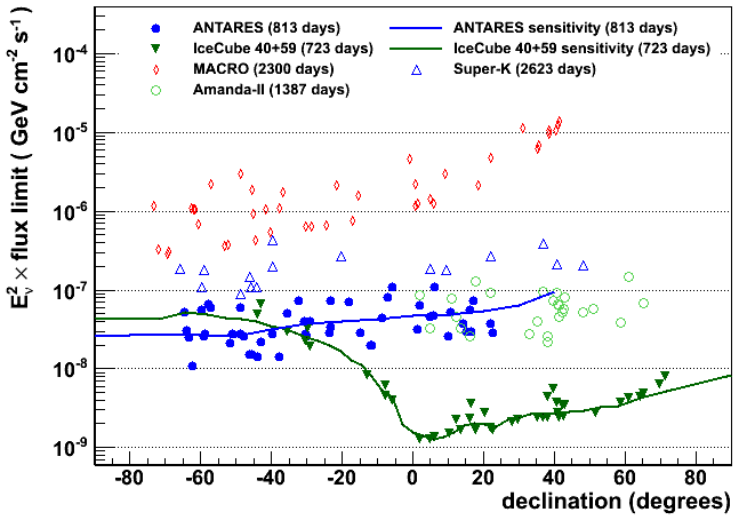

Figure 8.6.: Upper limits set on the normalisation of a neutrino flux proportional to E_ν^{-2} for the 51 candidate sources considered (see also Table 8.2). For a comparison, upper limits from other neutrino experiments are also included [161, 162, 163, 164]. The sensitivity of the analysis is shown as a solid line.

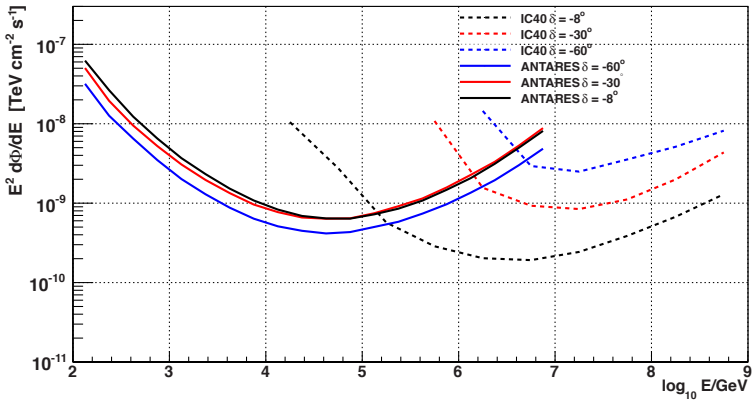

Figure 8.7.: Neutrino flux needed for a 5σ discovery as a function of the neutrino energy for ANTARES (solid line) and IceCube (dashed line) for three declinations in the Southern sky. In this plot, the discovery potential for IceCube with a 40 strings configuration is shown [59].

8.3. Limits on models of astrophysical neutrino emission

In Chapter 2 we presented three Galactic objects which are considered as promising sources of cosmic rays and neutrinos: RX J1713.7-3946, Vela X and the Crab Nebula. These sources are included in the candidate list search and 90% CL upper limits on the normalisation of a neutrino flux proportional to E_ν^{-2} was derived in the previous section.

We now present 90%CL upper limits on the flux normalisation obtained by assuming the models of astrophysical neutrino emission based on gamma-ray flux presented in Chapter 2. For RX J1713.7-3946 and Vela X the measured source extension is taken into account as explained in Section 7.7. Results are shown in Table 8.3 and Figure 8.8 in terms of the Model Rejection Factor (MRF) [165], i.e. the ratio between the 90% CL upper limit and the expected number of signal events. Since the MRF is > 1, the results are not sensitive enough to exclude the models. For RX J1713.7-3949 and Vela X, the limits derived are the most restrictive for the emission models considered.

Source	$\mu_{\rm s}^{90\%CL}$(PNT,E_ν^{-2})	Models	$\mu_{\rm s}^{90\%CL}$ (EXT)	MRF
RX J1713.7-3946	1.88	Kistler & Beacom	1.00	3.8
		Kappes et al.	1.11	8.8
		Morlino et al.	1.07	9
Vela X	1.29	Kistler & Beacom	1.25	3.1
		Kappes et al.	1.25	9.1
		Villante & Vissani	1.47	2.6
Crab	1.57	Kistler & Beacom	1.17	12
		Kappes et al.	1.95	37
		Amato et al.	2.02	26

Table 8.3.: Upper limits on the mean number of signal events, $\mu_{\rm s}$, expected from models of astrophysical neutrino emission for the three sources considered. Also shown are the upper limits on $\mu_{\rm s}$ obtained for the candidate list search which assumes a point-like source and a neutrino flux proportional to E_ν^{-2} (second column). The last column shows the MRF derived.

8.4. KM3NeT

The KM3NeT consortium recently started the construction of a multi-km^3 size neutrino telescope in the Mediterranean Sea [166]. The larger size of KM3NeT will make possible to investigate the Galactic plane with a much better sensitivity than ANTARES.

The expected number of events from RX J1713.7-3946 and Vela X assuming the model from Kappes et al. is shown in Table 8.4. Roughly 6 and 8 years of data taking are required for a 5σ discovery for RX J1713-3946 and Vela X respectively [167, 168].

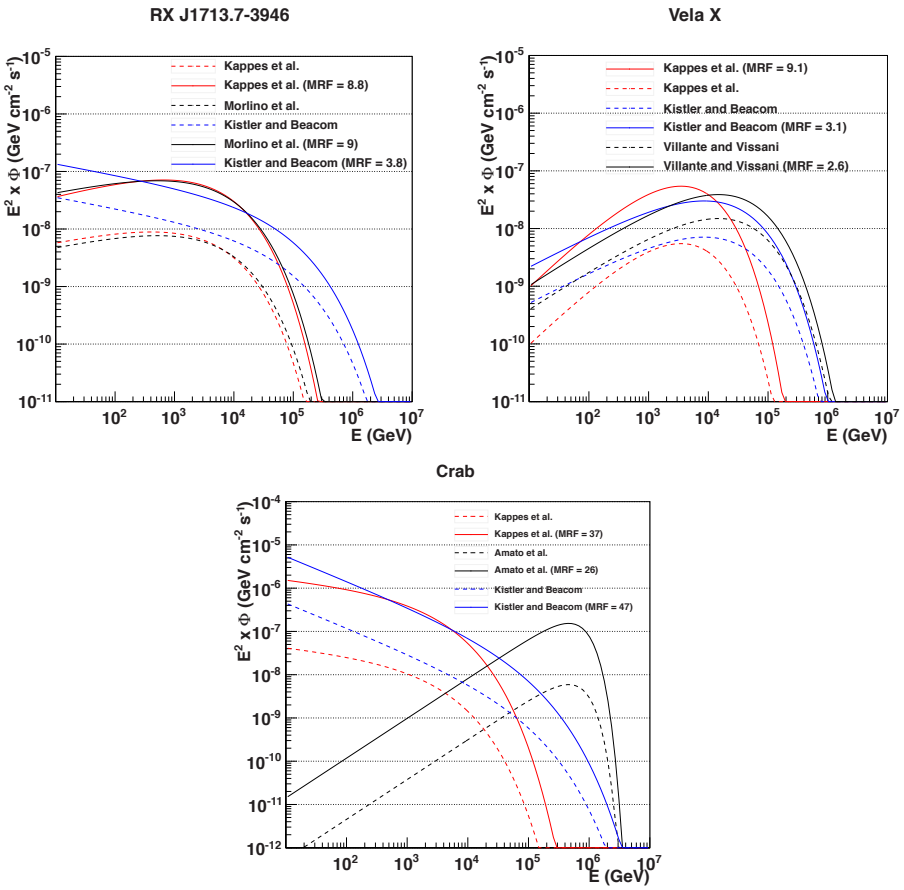

Figure 8.8.: For each of the models of astrophysical neutrino emission described in Section 2 (solid lines), an upper limit has been derived (dashed lines). The sources considered are RX J1713.7-3946 (top left), Vela X (top right) and the Crab SNR (bottom). More detailed results are reported in Table 8.3.

Source	$N_{\rm s}$	$N_{\rm b}$	$N_{\rm yr}^{5\sigma}$
RX J1713.7-3946	30	27	5.8
Vela X	25	23	7.5

Table 8.4.: Number of signal (second column) and background events (third column) according to the Kappes et al. model expected with the KM3Net detector. The last column shows the expected number of years of data taking needed for a 5σ discovery.

8.5. Conclusions and outlook

A search for cosmic neutrino point sources has been presented using data taken from 2007 to 2010 with the ANTARES telescope. A likelihood ratio method has been used in order to search for an excess of signal events over the background composed by atmospheric neutrinos and atmospheric muons. In addition to the position of the reconstructed events, the likelihood takes into account the information of the number of hits as an estimate of the neutrino energy. This improves the discovery potential by roughly 25%.

Two searches have been performed:

- **Full-sky search.** No statistically significant excess of signal has been found. The most signal-like cluster is located at $(\alpha, \delta) = (-46.5^\circ, -65^\circ)$ where 9 signal events are withing a 3 degrees cone. The likelihood fit assigns $\mu_s = 5.1$. The test statistic for this cluster is $\mathcal{Q} = 13.1$ which yields to a p-value of 2.6% with a significance of 2.2σ (two-sided convention).

- **Candidate list search.** The most signal-like source in the candidate list search is HESS J1023-575. The post-trial p-value is 41%, compatible with a background fluctuation. Since no significant excess of events was found, 90% CL upper limits were derived using the FC prescription. For some of the sources in the Southern sky, these limits are at the time of writing the most restrictive, assuming a neutrino flux proportional to E_ν^{-2}.

In this thesis, we also investigated the discovery potential for a neutrino flux model with an exponential cut-off and the inclusion of a possible source extension in the likelihood algorithm. These studies yield to the results presented in Section 7.7. Limits for specific models of astrophysical neutrino emission which deviates from the standard E^{-2} spectrum were computed for three sources: RX J1713.7-3946, Vela X and the Crab SNR. For some of the models considered, the results obtained are the most stringent.

A potential improvement for this analysis is the inclusion of shower events, originating from electron and tau neutrinos, will guarantee a significant improvement in terms of discovery probability ($\sim$ 30% assuming an optimistic $1/3$ as ratio between shower and muon events and 1% contribution from the muon neutrinos background) [169]. Another aspect which would be worth to investigate is the extension of the search to downgoing events [174]. The huge amount of background due to cosmic rays can be reduced by an energy selection (atmospheric muons and neutrinos have a softer spectrum compared to astrophysical neutrinos). The extension of the field of view with the selection of high-energy events would guarantee the possibility to search neutrinos from two very interesting SNRs: Cassiopea A and Tycho. For both sources, the gamma-ray data are well fitted by functions derived from hadronic models [170, 171] and a flux of neutrinos is expected [172].

Finally, a "stacking" search of astrophysical neutrinos from SNRs associated with giant molecular clouds would give interesting results. In Section 1.3 we have reported the recent results from the Fermi-LAT collaboration which identify the SNRs associated with giant molecular clouds IC 443 and W44 as sources of cosmic rays. There are however other sources of the same type whose gamma-ray emission seems to be well described by hadronic

models. Models describing the neutrino emission from these sources have been proposed in [172, 173], unfortunately the flux derived is well below the ANTARES sensitivity. A stacking analysis has the opportunity to search for cosmic neutrinos from this particular type of sources only, with the advantage to improve the significance of the neutrino signal from all sources which is proportional to $\sum_{i=1}^{N} S_i / \sqrt{\sum_{i=1}^{N} B_i}$ where N is the total number of sources, S_i the expected signal from the i-th source and B the total background.

The predicted neutrino flux from these sources assuming the model by Mandelartz and Becker Tjus [173] is shown in Figure 8.9. For comparison the ANTARES E_ν^{-2} upper limits derived for W28, W44, IC443 and W51C are also shown.

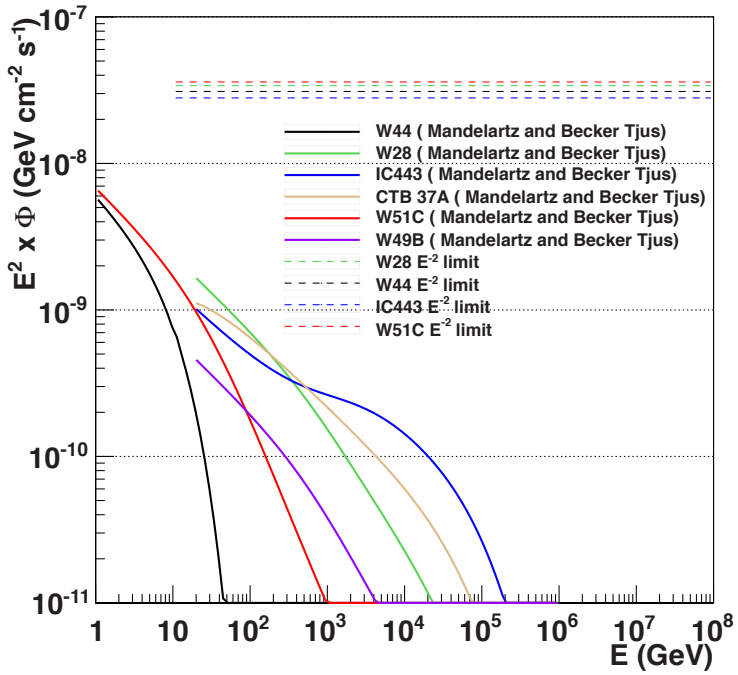

Figure 8.9.: Neutrino flux expected from six supernova remnants associated with giant molecular clouds assuming the model proposed by Mandelartz and Becker Tjus. For W28, W44, IC443 and W51 the ANTARES E_ν^{-2} upper limits are also shown.